ACADEMIC PRESS

Available online at www.sciencedirect.com

SCIENCE DIRECT®

Journal of Sound and Vibration 271 (2004) 905–920

JOURNAL OF SOUND AND VIBRATION

www.elsevier.com/locate/jsvi

Dynamics of a piecewise linear system subjected to a saturation constraint

J.C. Ji*

Institute of Mechanics AG2, Darmstadt University of Technology, Hochschulstr. 1, D-64289 Darmstadt, Germany

Received 10 June 2002; accepted 12 March 2003

Abstract

The dynamics of a periodically forced single-degree-of-freedom linear system with a proportional feedback control subjected to a saturation constraint is investigated in detail. Emphasis is placed on the determination of a double-entering saturation region per cycle periodic motion. Symmetric period-one solutions are derived analytically and their stability characteristics are determined. Other kinds of solutions such as asymmetric, subharmonic and chaotic solutions as well as multiple-crossing saturation region per cycle periodic solutions, found through numerical simulations, are also presented.

1. Introduction

An important aspect of the control system design is to choose the size of the actuator, such as the power required and the saturation level of the device. Generally, higher saturation levels require bigger and more costly actuators. On the other hand, the addition of a saturation element following a controller with an attempt to guarantee equipment reliability is a useful practice in almost all controlled systems. A key technical issue that needs to be addressed in these systems is the effect of the saturation constraints on the control systems' performance [1,2].

Saturation constraints may also occur in some typical electromechanical systems, for example, in an active magnetic bearing system. A typical magnetic bearing system is essentially composed of four components; sensors, controllers, power amplifiers, and electromagnetic actuators [3]. In this practical system, saturation phenomena could happen in several ways. The saturation of the magnetic material is achieved when all of the domains in the ferromagnetic core material are

*Corresponding author. School of Mechanical Engineering, The University of Adelaide, Adelaide, SA 5005, Australia. Tel.: +61-8-8303-6941; fax: +61-8-8303-4367.

E-mail address: jchji2@hotmail.com (J.C. Ji).

0022-460X/$ - see front matter
doi:10.1016/S0022-460X(03)00759-4

completely aligned with an external field. Further increases in the applied field produce only an equal gain in the centre field. This fixed value gain is determined not by the applied field but by the strengths of the internal dipoles. On the other hand, the saturation of the power amplifier can be caused by technical limitations of the amplifier. In addition, the limitation of the control current within a certain proper range is needed to prevent the hardware from being damaged. An occurrence of the saturation may lead to a poor dynamical behaviour of the system. For a controlled system with a saturation constraint, an in-depth knowledge of the system response can be of prime importance to design and control the system and to avoid unacceptable levels of vibration and noise.

In the context of control engineering, a large number of stable dynamical processes and engineering problems can be modelled via a standard linear second order system. The control of such a system has been completely solved [1,2]. However, the steady state response and its stability of the overall controlled system, in which a periodic excitation and a saturation constraint are presented, have not yet been studied in detail and need to be investigated. Due to the presence of saturation constraints, the equations governing the motions of such systems are inherently non-linear with piecewise linear characteristics. Although the dynamics of piecewise linear systems in connection with mostly impact oscillators has been the subject of many papers [e.g. Refs. [4–9]], the dynamics of the specific system considered here has not yet been investigated, to the author's knowledge.

The objective of the present study is to determine analytically the periodic motions of a harmonically excited single-degree-of-freedom (s.d.o.f.) linear system subjected to a saturation constraint, which occurs in the feedback control loop. In Section 2, the equations of motion are derived for a periodically forced s.d.o.f. piecewise linear system. A symmetric period-one solution is considered in Section 3, and its stability characteristic is examined in Section 4. Other kinds of solutions, such as asymmetric, subharmonic periodic and chaotic motions, are briefly given in Section 5. Finally, conclusions are presented in Section 6.

2. Equations of motion

The mathematical model to be considered in the present paper is generalized from a specific example of engineering systems, i.e., a Jeffcott rotor–magnetic bearing system. However, the equations of motion can also be used to model mathematically a class of simple control systems subjected to various saturation constraints in the feedback control signal. Consider a Jeffcott rotor–magnetic bearing system subjected to an unbalanced excitation. The equations of motion for the shaft motion in the horizontal direction can be described as [10]

$$mx'' + cx' + kx = F_{mb} + me\Omega^2 \cos \Omega T, \tag{1}$$

where m is the mass of the rotor, c is the damping coefficient, k is the shaft stiffness, e is the mass eccentricity, F_{mb} represents the magnetic force, Ω is the rotational speed, and the prime denotes differentiation with respect to the physical time T.

When the saturation constraints are taken into account, the magnetic force generated by the magnetic bearing cannot increase to infinity but is constrained within a certain range. The maximum upper force is reached when any saturation phenomenon occurs. The magnetic force

with the saturation constraints can be written as

$$F_{mb} = \frac{1}{2}(|F(x,i) + F_s| - |F(x,i) - F_s|). \tag{2}$$

where F_s denotes the upper limit force, $F(x,i)$ represents the magnetic force under a normal operating situation and is non-linear in nature. As a matter of convenience, only the linear approximate form is used to simplify the force according to the expression given in Refs. [3,11],

$$F(x,i) = k_i i - k_x x, \tag{3}$$

where i denotes the control current, k_i is the actuator gain and k_x is the open loop stiffness. For simplicity, the feedback control system is assumed to generate a current that is proportional to the rotor displacement, i.e., a P-controller, with the form $i = px$, where p represents the proportional gain. Without loss of generality, it is also assumed that the saturation constraint is indicated by simply restricting the displacement x, and the upper level of the saturation is presented by x_s. In terms of x and x_s, the upper saturation value of the magnetic force can be expressed as $F_s = k_c x_s$, where $k_c = k_i p - k_x$. The overall magnetic force is of the form shown in Fig. 1.

Substituting Eq. (2) into Eq. (1), and introducing non-dimensional variables by $x = x_s y$ and $t = \Omega_1 T$, yields the equations of motion in the non-dimensional form

$$\ddot{y} + 2\delta\dot{y} + y + \omega_2^2 y = f\cos\omega t \quad \text{for } |y| \leqslant 1, \tag{4a}$$

$$\ddot{y} + 2\delta\dot{y} + y + \omega_2^2\,\mathrm{sgn}(y) = f\cos\omega t \quad \text{for } |y| \geqslant 1, \tag{4b}$$

where $\Omega_1^2 = k/m$, $2\delta = c/m\Omega_1$, $\omega_2^2 = k_c/k$, $\omega = \Omega/\Omega_1$, $f = e\omega^2/x_s$, $\mathrm{sgn}(\cdot)$ denotes the sign function, and the superscript dot indicates differentiation with respect to the non-dimensional time t. For a small amplitude response, the controller and actuator operate under a normal situation. The saturation constraint does not need to be considered. The system is entirely linear and behaves according to the solution of Eq. (4a). This case is not considered in the present paper as the system demonstrates only small amplitude linear harmonic motions. However, for the amplitude of response larger than the level of saturation, the dynamical behaviour of the system is locally governed by Eq. (4b). An overall behaviour of the system is then determined by joining

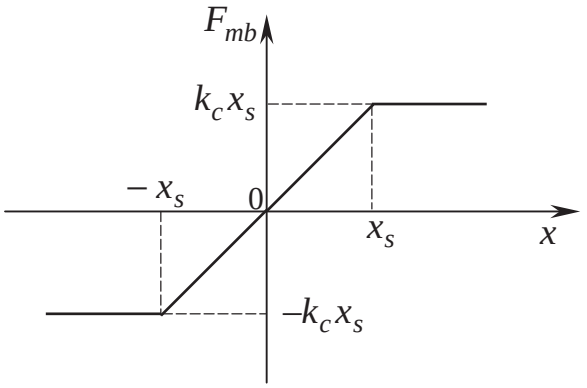

Fig. 1. The symmetric, piecewise linear magnetic force in the presence of saturation constraints.

Eqs. (4a) and (4b) together. The motions of the system will enter the saturation regions at least once in one period of a periodic motion.

3. Symmetric period-one solutions

It is easy to note that system (4) is continuous and satisfies the Lipschitz condition. Therefore, the solution of Eq. (4) exists and is unique. However, it cannot be obtained in closed form, since, as will be seen, the times of passing through the boundaries of the saturation region cannot be found explicitly. The results of numerical simulations on the dynamical behaviour of system (4) suggested that the system may exhibit symmetric, asymmetric, subharmonic periodic motions, and chaotic motions. In addition, single-, double- and multiple-crossing saturation region per cycle periodic solutions were also found to exist in some combinations of the system parameters. In the present work, a strong emphasis is placed on the analytical determination of the double-entering saturation region per cycle symmetric period-one solutions. Such a typical period-one solution is shown in Fig. 2. The response consists entirely of four distinct segments of the motion according to four time intervals; $[t_0, t_1]$, $[t_1, t_2]$, $[t_2, t_3]$ and $[t_3, t_4]$, where $t_4 = t_0 + 2\pi/\omega$, and $t_{i-1}(i = 1, 2, 3, 4)$ denotes the time instant that the motion crosses the boundaries of the saturation regions. The construction of the solution is based on the observation that Eq. (4) is linear in each of the regions $|y(t)| \leqslant 1$ and $|y(t)| \geqslant 1$ respectively. Due to the symmetry of the solution being sought, only two parts of the motion need to be considered.

Let $y_1(t)$ denote the solution starting from time t_0 in the region $y(t) \geqslant 1$, and $y_2(t)$ from t_1 in $|y(t)| \leqslant 1$, then the general solutions can be written as

$$\begin{aligned} y_1(t) &= e^{-\delta(t-t_0)}[A_1 \cos \beta_1(t - t_0) + B_1 \sin \beta_1(t - t_0)] + G_1 \sin \omega t \\ &\quad + H_1 \cos \omega t + Y_0 \text{ for } y_1(t) \geqslant 1, \\ y_2(t) &= e^{-\delta(t-t_1)}[A_2 \cos \beta_2(t - t_1) + B_2 \sin \beta_2(t - t_1)] + G_2 \sin \omega t \\ &\quad + H_2 \cos \omega t \text{ for } |y_2(t)| \leqslant 1, \end{aligned} \tag{5}$$

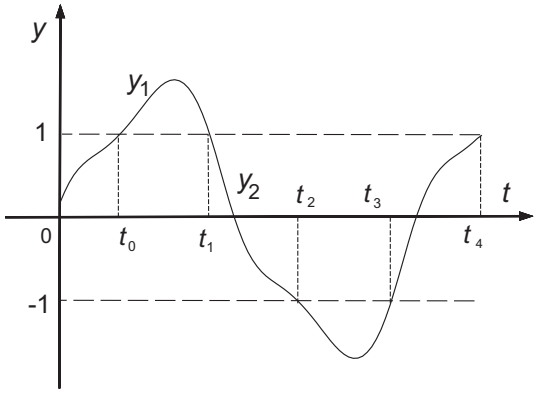

Fig. 2. The double-entering saturation region per cycle symmetric period-one solution.

and the corresponding velocities as

$$\dot{y}_1(t) = e^{-\delta(t-t_0)}[(\beta_1 B_1 - \delta A_1)\cos\beta_1(t-t_0) - (\beta_1 A_1 + \delta B_1)\sin\beta_1(t-t_0)] + \omega G_1 \cos\omega t - \omega H_1 \sin\omega t \quad \text{for } y_1(t) \geqslant 1,$$

$$\dot{y}_2(t) = e^{-\delta(t-t_1)}[(\beta_2 B_2 - \delta A_2)\cos\beta_2(t-t_1) - (\beta_2 A_2 + \delta B_2)\sin\beta_2(t-t_1)] + \omega G_2 \cos\omega t - \omega H_2 \sin\omega t \quad \text{for } |y_2(t)| \leqslant 1, \tag{6}$$

where $\beta_1 = \sqrt{1-\delta^2}$, $\beta_2 = \sqrt{1+\omega_2^2-\delta^2}$, $Y_0 = -\omega_2^2 \operatorname{sgn}(y)$,

$$G_1 = \frac{2\delta\omega f}{(1-\omega^2)^2 + (2\delta\omega)^2}, \quad H_1 = \frac{(1-\omega^2)f}{(1-\omega^2)^2 + (2\delta\omega)^2},$$

$$G_2 = \frac{2\delta\omega f}{(1+\omega_2^2-\omega^2)^2 + (2\delta\omega)^2}, \quad H_2 = \frac{(1+\omega_2^2-\omega^2)f}{(1+\omega_2^2-\omega^2)^2 + (2\delta\omega)^2}.$$

Here, it has been assumed that the steady state response starts at time instant t_0 from $y_1(t_0) = 1$ and stays thereafter in the saturation region $y_1(t) \geqslant 1$ till moment t_1. Since the origin of the starting time has been set by the choice of the forcing term in Eq. (5), it is not possible to set $t_0 = 0$. At this point it is clear that there are six unknowns of the problem at hand, that is, four constants A_1, B_1, A_2 and B_2, and two crossing times t_0 and t_1. These constants can be determined by imposing an appropriate set of initial, periodicity, continuity and symmetry conditions. These conditions can be expressed as follows:

$$y_1(t_0) = 1, \quad y_1(t_1) = 1, \quad y_2(t_1) = 1, \quad \dot{y}_1(t_1) = \dot{y}_2(t_1),$$
$$y_2(t_2) = -1, \quad \dot{y}_2(t_2) = -\dot{y}_1(t_0), \quad t_2 - t_0 = \pi/\omega. \tag{7}$$

Here, the last two conditions arise from the symmetry of the double-crossing saturation region per cycle symmetric period-one solutions being examined. The unknown constants A_1, B_1, A_2 and B_2, as functions of the system parameters and the crossing times t_0 and t_1, can be determined by substituting Eq. (5) into four displacement conditions given by Eq. (7). For the clarity of notation, these constants are denoted as

$$A_i = A_{i0} + A_{ic}\cos\omega t_0 + A_{is}\sin\omega t_0,$$
$$B_i = B_{i0} + B_{ic}\cos\omega t_0 + B_{is}\sin\omega t_0, \quad i = 1, 2. \tag{8}$$

with $A_{10} = 1 - Y_0$, $A_{1c} = -H_1$, $A_{1s} = -G_1$, $A_{20} = 1$, $A_{2c} = -G_2 s_{10} - H_2 c_{10}$,

$$A_{2s} = H_2 s_{10} - G_2 c_{10}, \quad B_{10} = [1 - Y_0 - c_{110}(1 - Y_0)e_{10}]/e_{10}s_{110},$$

$$B_{1c} = (e_{10}c_{110}H_1 - s_{10}G_1 - c_{10}H_1)/e_{10}s_{110},$$
$$B_{1s} = (e_{10}c_{110}G_1 - c_{10}G_1 + s_{10}H_1)/e_{10}s_{110},$$

$$B_{20} = -[e_{10} + (c_2 c_{210} + s_2 s_{210})e_0]/e_0(s_2 c_{210} - c_2 s_{210}),$$

$$B_{2c} = [e_{10}H_2 - e_0 A_{2c}(c_2 c_{210} + s_2 s_{210})]/e_0(s_2 c_{210} - c_2 s_{210}),$$

$$B_{2s} = [e_{10}G_2 - e_0 A_{2s}(c_2 c_{210} + s_2 s_{210})]/e_0(s_2 c_{210} - c_2 s_{210}),$$

where

$$s_1 = \sin\beta_1\frac{\pi}{\omega}, \quad c_1 = \cos\beta_1\frac{\pi}{\omega}, \quad s_2 = \sin\beta_2\frac{\pi}{\omega}, \quad c_2 = \cos\beta_2\frac{\pi}{\omega},$$

$$s_{10} = \sin\omega(t_1 - t_0), \quad c_{10} = \cos\omega(t_1 - t_0), \quad s_{110} = \sin\beta_1(t_1 - t_0),$$
$$c_{110} = \cos\beta_1(t_1 - t_0),$$

$$s_{210} = \sin\beta_2(t_1 - t_0), \quad c_{210} = \cos\beta_2(t_1 - t_0), \quad e_0 = e^{-\delta\pi/\omega}, \quad e_{10} = e^{-\delta(t_1 - t_0)}.$$

In order to obtain the solutions $y_1(t)$ and $y_2(t)$, it is naturally necessary to find the crossing times t_1 and t_0. Substituting expression (8) into Eq. (6) and the resulting velocities into two velocity conditions given by Eq. (7), yields the following two transcendental equations for the time interval $(t_1 - t_0)$ and time instant t_0 as

$$\begin{aligned} D_{11}\cos\omega t_0 + D_{12}\sin\omega t_0 &= D_{10}, \\ D_{21}\cos\omega t_0 + D_{22}\sin\omega t_0 &= D_{20}, \end{aligned} \tag{9}$$

with $D_{11} = a_{11}B_{1c} + a_{12}A_{1c} + a_{13}$, $D_{12} = a_{11}B_{1s} + a_{12}A_{1s} + a_{14}$,

$$D_{10} = \beta_2 B_{20} - \delta A_{20} - a_{11}B_{10} - a_{12}A_{10},$$

$$D_{21} = (\beta_2 B_{2c} - \delta A_{2c})a_{21} + (\beta_2 A_{2c} + \delta B_{2c})a_{22} + a_{23},$$

$$D_{22} = (\beta_2 B_{2s} - \delta A_{2s})a_{21} + (\beta_2 A_{2s} + \delta B_{2s})a_{22} + a_{24},$$

$$D_{20} = \beta_1 B_{10} - \delta A_{10} + (\beta_2 B_{20} - \delta A_{20})a_{21} + (\beta_2 A_{20} + \delta B_{20})a_{22},$$

where $a_{11} = e_{10}c_{110}\beta_1 - e_{10}s_{110}\delta$, $a_{12} = -e_{10}c_{110}\delta - e_{10}s_{110}\beta_1$,

$$a_{13} = \omega(G_1 - G_2)c_{10} - \omega(H_1 - H_2)s_{10} + \delta A_{2c} - \beta_2 B_{2c},$$

$$a_{14} = \omega(G_2 - G_1)s_{10} - \omega(H_1 - H_2)c_{10} + \delta A_{2s} - \beta_2 B_{2s},$$

$$a_{21} = e_0(c_2 c_{210} + s_2 s_{210})/e_{10}, \quad a_{22} = e_0(c_2 s_{210} - s_2 c_{210})/e_{10},$$

$$a_{23} = \omega(G_1 - G_2) + \beta_1 B_{1c} - \delta A_{1c}, \quad a_{24} = \omega(H_2 - H_1) + \beta_1 B_{1s} - \delta A_{1s}.$$

Separating $\sin\omega t_0$ and $\cos\omega t_0$ in terms of the system parameters and the time interval $(t_1 - t_0)$ from Eq. (9) yields

$$\cos\omega t_0 = \frac{(D_{10}D_{22} - D_{12}D_{20})}{(D_{11}D_{22} - D_{12}D_{21})}, \quad \sin\omega t_0 = \frac{(D_{11}D_{20} - D_{10}D_{21})}{(D_{11}D_{22} - D_{12}D_{21})}. \tag{10}$$

Applying the trigonometric identity, $\sin^2\omega t_0 + \cos^2\omega t_0 = 1$, leads to a transcendental equation

$$(D_{10}D_{22} - D_{12}D_{20})^2 + (D_{11}D_{20} - D_{10}D_{21})^2 = (D_{11}D_{22} - D_{12}D_{21})^2. \tag{11}$$

This equation involves only the system parameters and the unknown time interval $(t_1 - t_0)$. It seems that no analytic solutions can be found to Eq. (11). Thus numerical means have to

be adopted to solve the equation. The value of t_0 can be obtained from Eq. (10) after getting the solutions to Eq. (11) in the range 0 to π/ω, and t_1 is found by a simple addition. Then the constants A_1, B_1, A_2 and B_2 can be evaluated from Eq. (8), and hence the corresponding histories of $y_1(t)$ and $y_2(t)$ can be calculated from Eq. (5). It should be noted that not all the possible solutions to Eq. (11) for the time interval $(t_1 - t_0)$ are physical and acceptable ones. Only one solution, which produces a trajectory in the saturation range (i.e., $y_1(t) \geqslant 1$), is the desirable solution. In Section 4, the stability of such a symmetric periodic solution will be studied.

4. Stability of the periodic solutions

Due to the presence of stiffness discontinuities in Eq. (4), the stability characteristic of a symmetric period-one motion cannot be examined using the usual method of the classical Floquet theory. An alternative approach [12] is applicable to investigate the asymptotic behaviour of the perturbations to the steady state solutions. The idea is to add small perturbations to the initial conditions and examine what happens to the resultant perturbed solutions as the motion progresses. The symmetry of the motion being examined ensures that its stability characteristic can be fully determined in one half of the response.

Let $z_1(t)$ and $z_2(t)$ denote the corresponding perturbed solutions to $y_1(t)$ and $y_2(t)$ respectively. The perturbed initial conditions for the perturbed motion of the first segment $z_1(t)$ can be written as

$$z_1(t_0 + \Delta t_0) = 1, \quad \dot{z}_1(t_0 + \Delta t_0) = v_0 + \Delta v_0,$$

where the operator Δ indicates a small perturbation of the operand. The corresponding perturbed solutions for the displacement and velocity can be expressed as

$$\begin{aligned} z_1(t) = {} & \mathrm{e}^{-\delta(t-t_0-\Delta t_0)}[P_1 \cos\beta_1(t - t_0 - \Delta t_0) + Q_1 \sin\beta_1(t - t_0 - \Delta t_0)] \\ & + G_1 \sin\omega t + H_1 \cos\omega t + Y_0 \quad \text{for } z_1(t) \geqslant 1, \end{aligned}$$

$$\begin{aligned} \dot{z}_1(t) = {} & \mathrm{e}^{-\delta(t-t_0-\Delta t_0)}[(\beta_1 Q_1 - \delta P_1)\cos\beta_1(t - t_0 - \Delta t_0) - (\beta_1 P_1 + \delta Q_1)\sin\beta_1(t - t_0 - \Delta t_0)] \\ & + \omega G_1 \cos\omega t - \omega H_1 \sin\omega t \quad \text{for } z_1(t) \geqslant 1. \end{aligned} \tag{12}$$

At time instant $t = t_1 + \Delta t_1$, the response reaches one boundary of the saturation region and will leave the saturation region thereafter. The perturbed response at the moment of departure is assumed to be

$$z_1(t_1 + \Delta t_1) = 1, \quad \dot{z}_1(t_1 + \Delta t_1) = v_1 + \Delta v_1. \tag{13}$$

Since the perturbations in the initial conditions are assumed to be small, it is expected that the coefficients P_1 and Q_1 will assume values close to those of the unperturbed motion, A_3 and B_3 respectively. To the first order, they are given by

$$\begin{aligned} P_1 &= A_3 + \frac{\partial A_3}{\partial t_0}\Delta t_0 + \frac{\partial A_3}{\partial v_0}\Delta v_0, \\ Q_1 &= B_3 + \frac{\partial B_3}{\partial t_0}\Delta t_0 + \frac{\partial B_3}{\partial v_0}\Delta v_0. \end{aligned} \tag{14}$$

The constants A_3 and B_3 are determined, without unnecessary complexity, by imposing the unperturbed initial conditions $z_1(t_0) = 1$ and $\dot{z}_1(t_0) = v_0$, which are given by

$$A_3 = 1 - Y_0 - G_1 \sin \omega t_0 - H_1 \cos \omega t_0,$$

$$B_3 = (v_0 + \delta A_3 - \omega G_1 \cos \omega t_0 + \omega H_1 \sin \omega t_0)/\beta_1. \tag{15}$$

Substituting expression (15) into Eq. (14) yields

$$P_1 = A_3 + A_{31}\Delta t_0, \quad Q_1 = B_3 + B_{31}\Delta t_0 + \Delta v_0/\beta_1, \tag{16}$$

where $A_{31} = \omega H_1 \sin \omega t_0 - \omega G_1 \cos \omega t_0$,

$$B_{31} = [\omega(\omega G_1 + \delta H_1) \sin \omega t_0 + \omega(\omega H_1 - \delta G_1) \cos \omega t_0]/\beta_1.$$

Substituting expressions (15) and (16) into Eq. (12) then the resultant equations into condition (13), and keeping only the first order terms gives rise to

$$K_{11}\Delta t_1 + K_{12}\Delta t_0 + K_{13}\Delta v_0 = 0,$$

$$\Delta v_1 = K_{21}\Delta t_1 + K_{22}\Delta t_0 + K_{23}\Delta v_0, \tag{17}$$

with $K_{11} = e_{10}F_{11} - e_{10}\delta(A_3 c_{110} + B_3 s_{110}) + \omega F_{13}$,

$$K_{12} = e_{10}F_{12} + e_{10}\delta(A_3 c_{110} + B_3 s_{110}), \quad K_{13} = e_{10}s_{110}/\beta_1,$$

$$K_{21} = e_{10}L_{13} - e_{10}\delta L_{10} - \omega^2 G_1 \sin \omega t_1 - \omega^2 H_1 \cos \omega t_1, \quad K_{22} = e_{10}L_{11} + e_{10}\delta L_{10}, \quad K_{23} = e_{10}L_{12},$$

where $F_{11} = B_3\beta_1 c_{110} - A_3\beta_1 s_{110}$, $F_{12} = A_3\beta_1 s_{110} + A_{31}c_{110} + B_{31}s_{110} - B_3\beta_1 c_{110}$,

$$F_{13} = G_1 \cos \omega t_1 - H_1 \sin \omega t_1, \quad L_{10} = (\beta_1 B_3 - \delta A_3)c_{110} - (\beta_1 A_3 + \delta B_3)s_{110},$$

$$L_{11} = (\beta_1 B_{31} - \delta A_{31})c_{110} + (\beta_1 B_3 - \delta A_3)\beta_1 s_{110} - (\beta_1 A_{31} + \delta B_{31})s_{110} + (\beta_1 A_3 + \delta B_3)\beta_1 c_{110},$$

$$L_{12} = c_{110} - \delta s_{110}/\beta_1, \quad L_{13} = (\delta A_3 - \beta_1 B_3)\beta_1 s_{110} - (\beta_1 A_3 + \delta B_3)\beta_1 c_{110}.$$

The asymptotic behaviour of the perturbed motion for the second segment of the response from time $(t_1 + \Delta t_1)$ to $(t_2 + \Delta t_2)$ can be investigated using the same procedure performed as that for the first segment. Similarly, the solutions corresponding to the perturbed initial conditions $z_2(t_1 + \Delta t_1) = 1$, $\dot{z}_2(t_1 + \Delta t_1) = v_1 + \Delta v_1$, can be written in the form

$$z_2(t) = e^{-\delta(t-t_1-\Delta t_1)}[P_2 \cos \beta_2(t - t_1 - \Delta t_1) + Q_2 \sin \beta_2(t - t_1 - \Delta t_1)] + G_2 \sin \omega t + H_2 \cos \omega t \quad \text{for } |z_2(t)| \leqslant 1,$$

$$\dot{z}_2(t) = e^{-\delta(t-t_1-\Delta t_1)}[(\beta_2 Q_2 - \delta P_2) \cos \beta_2(t - t_1 - \Delta t_1) - (\beta_2 P_2 + \delta Q_2) \sin \beta_2(t - t_1 - \Delta t_1)] + \omega G_2 \cos \omega t - \omega H_2 \sin \omega t \quad \text{for } |z_2(t)| \leqslant 1. \tag{18}$$

The constants P_2 and Q_2 to the first order are given by

$$P_2 = A_4 + A_{41}\Delta t_1, \quad Q_2 = B_4 + B_{41}\Delta t_1 + \Delta v_1/\beta_2, \tag{19}$$

where $A_4 = 1 - G_2 \sin \omega t_1 - H_2 \cos \omega t_1$, $A_{41} = \omega H_2 \sin \omega t_1 - \omega G_2 \cos \omega t_1$,

$$B_4 = (v_1 + \delta A_2 - \omega G_2 \cos \omega t_1 + \omega H_2 \sin \omega t_1)/\beta_2,$$

$$B_{41} = [\omega(\omega H_2 - \delta G_2) \cos \omega t_1 + \omega(\delta H_2 + \omega G_2) \sin \omega t_1]/\beta_2.$$

The perturbed response at moment $(t_2 + \Delta t_2)$ is assumed to be

$$z_2(t_2 + \Delta t_2) = 1, \quad \dot{z}_2(t_2 + \Delta t_2) = v_2 + \Delta v_2. \tag{20}$$

Substituting Eq. (18) into condition (20) and performing some algebraic manipulations yields the following equations retaining terms up to the first order as

$$M_{11}\Delta t_2 + M_{12}\Delta t_1 + M_{13}\Delta v_1 = 0,$$

$$\Delta v_2 = M_{21}\Delta t_2 + M_{22}\Delta t_1 + M_{23}\Delta v_1, \tag{21}$$

with $M_{11} = e_0F_{21}/e_{10} - \delta(A_4c_{201} + B_4s_{201})e_0/e_{10} + F_{23}\omega$,

$$M_{12} = e_0F_{22}/e_{10} + \delta(A_4c_{201} + B_4s_{201})e_0/e_{10}, \quad M_{13} = e_0s_{201}/e_{10}\beta_2,$$

$$M_{21} = e_0L_{23}/e_{10} - e_0\delta L_{20}/e_{10} + \omega^2G_2\sin\omega t_0 + \omega^2H_2\cos\omega t_0,$$

$$M_{22} = e_0L_{21}/e_{10} + e_0\delta L_{20}/e_{10}, \quad M_{23} = e_0L_{22}/e_{10},$$

where $F_{21} = B_4\beta_2c_{201} - A_4\beta_2s_{201}$, $F_{22} = A_4\beta_2s_{201} + A_{41}c_{201} + B_{41}s_{201} - B_4\beta_2c_{201}$,

$$F_{23} = H_2\sin\omega t_0 - G_2\cos\omega t_0, \quad L_{20} = (\beta_2B_4 - \delta A_4)c_{201} - (\beta_2A_4 + \delta B_4)s_{201},$$

$$L_{21} = (\beta_2B_4 - \delta A_4)\beta_2s_{201} + (\beta_2B_{41} - \delta A_{41})c_{201} - (\beta_2A_{41} + \delta B_{41})s_{201} + (\beta_2A_4 + \delta B_4)\beta_2c_{201},$$

$$L_{22} = c_{201} - \delta s_{201}/\beta_2, \quad L_{23} = (\delta A_4 - \beta_2B_4)\beta_2s_{201} - (\beta_2A_4 + \delta B_4)\beta_2c_{201},$$

$$c_{201} = \cos\beta_2\left(\frac{\pi}{\omega} + t_0 - t_1\right), \quad s_{201} = \sin\beta_2\left(\frac{\pi}{\omega} + t_0 - t_1\right).$$

Eqs. (17) and (21) can be put in matrix form as follows:

$$\begin{bmatrix}\Delta t_1\\ \Delta v_1\end{bmatrix} = \mathbf{R}\begin{bmatrix}\Delta t_0\\ \Delta v_0\end{bmatrix}, \begin{bmatrix}\Delta t_2\\ \Delta v_2\end{bmatrix} = \mathbf{U}\begin{bmatrix}\Delta t_1\\ \Delta v_1\end{bmatrix}, \tag{22}$$

where $\mathbf{R}$ is the (2×2) matrix with the entries $r_{11} = -K_{12}/K_{11}$, $r_{12} = -K_{13}/K_{11}$, $r_{21} = K_{22} - K_{21}K_{12}/K_{11}$, $r_{22} = K_{23} - K_{21}K_{13}/K_{11}$ respectively. And $\mathbf{U}$ denotes the (2×2) matrix with the elements $u_{11} = -M_{12}/M_{11}$, $u_{12} = -M_{13}/M_{11}$, $u_{21} = M_{22} - M_{21}M_{12}/M_{11}$, $u_{22} = M_{23} - M_{21}M_{13}/M_{11}$ respectively.

The small perturbations of the symmetric solution during the first half period are obtained by combining the two equations given by Eq. (22) to form an equation

$$\begin{bmatrix}\Delta t_2\\ \Delta v_2\end{bmatrix} = \mathbf{J}\begin{bmatrix}\Delta t_0\\ \Delta v_0\end{bmatrix}, \tag{23}$$

where $\mathbf{J}$ represents the transition matrix for the response from moment $(t_0 + \Delta t_0)$ to $(t_2 + \Delta t_2)$, and is given by $\mathbf{J} = \mathbf{RU}$. The stability of the steady state solution is determined by the eigenvalues of this transition matrix. Denote the trace of $\mathbf{J}$ by TJ and the determinant of $\mathbf{J}$ by DJ, then two eigenvalues of the matrix are given by

$$\lambda_{1,2} = \tfrac{1}{2}[TJ \pm (TJ^2 - 4DJ)^{1/2}]. \tag{24}$$

The symmetric period-one motion is asymptotically stable if both eigenvalues λ_1, λ_2 of matrix $\mathbf{J}$ have modulus less than unity. When either of two eigenvalues has modulus greater than one the

solution is unstable. From the preceeding discussion, it is known that all the elements of matrix **J** are functions of the system parameters and the crossing times which cannot be given explicitly. This means that it is not possible to get explicit expressions in terms of the system parameters for the trace and determinant of matrix **J**. In fact, a major difficulty is in developing a simple expression for the trace TJ. Nevertheless, by substituting the expressions of the elements of matrices **R** and **U** and performing some algebraic manipulations, the determinants of matrices **R** and **U**, namely DR and DU, are eventually expressed in a simple form as

$$DR = e_{10}^2 \frac{\dot{y}_1(t_0)}{\dot{y}_1(t_1)}, \quad DU = \frac{e_0^2}{e_{10}^2} \frac{\dot{y}_2(t_1)}{\dot{y}_2(t_2)}. \tag{25}$$

The determinant of matrix **J** is then given by the product of the traces of matrices **R** and **U** as

$$DJ = e_0^2 \frac{\dot{y}_1(t_0)}{\dot{y}_1(t_1)} \cdot \frac{\dot{y}_2(t_1)}{\dot{y}_2(t_2)}. \tag{26}$$

By imposing the continuity and periodicity conditions of the symmetric solution, i.e., $\dot{y}_1(t_1) = \dot{y}_2(t_1)$, $\dot{y}_2(t_2) = -\dot{y}_1(t_0)$, Eq. (26) is further simplified to a quite simple form

$$DJ = -e_0^2. \tag{27}$$

Therefore, if the damping coefficient δ in Eq. (4) is positive, it is obvious from Eq. (27) that $-1 < DJ < 0$. This indicates that no Hopf bifurcation is possible in the symmetric motion examined. As the system parameters are changed, the modulus of one eigenvalue may take the value of unity, where a bifurcation occurs. One possible way for the eigenvalue to cross the unit circle is through $+1$, which corresponds to a saddle-node, pitchfork or transcritical bifurcation. The other way is through -1, which relates to a period-doubling bifurcation. The stability boundaries $\lambda = \pm 1$ can be established by solving the equation

$$DJ \mp TJ + 1 = 0. \tag{28}$$

It is noted that Eq. (28) involves trigonometric and exponential function terms which depend on the crossing times t_1 and t_0. This implies that the stability diagrams cannot be analytically built up. In addition, since the determination of t_1 and t_0 depends on the roots of transcendental equation(11), a numerical construction of the stability diagrams will be an extremely laborious task. The stability diagrams are not pursued in the present paper.

To validate the present analytical results, the symmetric period-one solutions determined by the present analysis were compared with those obtained by the direct numerical integration for several cases. The classical fourth order *Runge–Kutta* algorithm was employed to perform the numerical integration to Eq. (4). It was found that the steady state solutions obtained by these two different means were identical. As an illustrative example, consider a system with the parameters $\delta = 0.25$, $\omega_2 = \sqrt{3}$, $f = 2.5$ and $\omega = 1.5$. For this combination of the system parameters, only a double-crossing symmetric motion exists under different sets of initial conditions. Two eigenvalues of transition matrix **J** calculated from Eq. (24) are $\lambda_1 \approx 0.5311$ and $\lambda_2 \approx -0.6608$, indicating that the steady state solution is stable. The present analysis given in Section 3 gives that $t_0 \approx 0.2825$ and $t_1 \approx 1.9923$. The values of crossing times t_0 and t_1 given by the numerical integration are nearly identical to those predicted by the developed analysis. A very small difference only in the fourth decimal place, which resulted from a run-out of the calculation, was found between the values obtained by the two different approaches. The phase portrait of the symmetric period-one

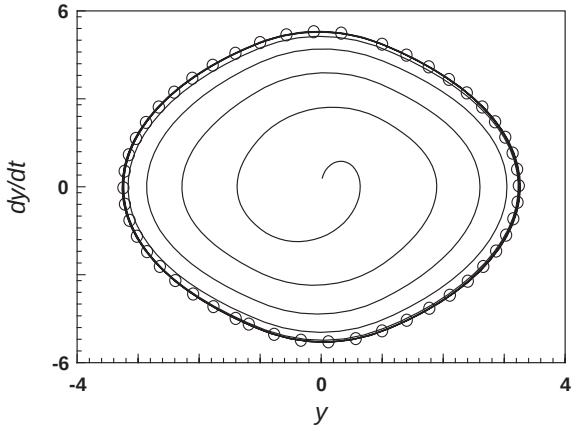

Fig. 3. The phase portrait of a double-crossing saturation region per cycle symmetric period-one solution; "—" the direct numerical integration results, and "°" the analytical results.

solution found by both the numerical integration and the developed analysis is shown in Fig. 3. The transient response of the system originating from initial conditions $(y_0, \dot{y}_0) = (0.0, 0.1)$, which was obtained from the numerical integration, converges quickly to the steady state response. The steady state motion is obviously in excellent agreement with that obtained by the developed analysis.

5. Other kinds of solutions

The analysis presented in Sections 3 and 4 can be extendible to determine asymmetric and subharmonic solutions, and even to determine the solutions having multiple-crossing saturation region per cycle. However, except single-crossing saturation region asymmetric solutions, the procedure in finding any other solutions will be exceptionally lengthy and involve many more algebraic manipulations. In this section, alternatively, some examples of the numerical simulations are given to illustrate other kinds of solutions.

The widely used software package MATLAB/SIMULINK was employed to simulate the dynamical system (4). This system model can be easily built up by the built-in SIMULINK blocks. The saturation block in the library of non-linear components was used to impose the upper and lower bounds (± 1) on the input signal. The fourth order *Runge–Kutta* procedure was chosen to be the numerical integration method of the ODE solvers. The initial conditions for two integrator blocks were all set to zero, unless otherwise stated. The simulation results were observed on-line during the dynamic simulation using scope and other display blocks. The numerical simulations were carried out under three sets of the forcing frequency $\omega < 1$, $1 \leqslant \omega \leqslant (1 + \omega_2^2)^{1/2}$, and $\omega > (1 + \omega_2^2)^{1/2}$. Due to a lack of analytical results to guide the simulations, the choice of system parameters and initial conditions was made arbitrarily. It was also not possible to assert the presence or absence of a certain solution in a given set of the system parameters, unless it was found by a fortuitous choice of initial conditions.

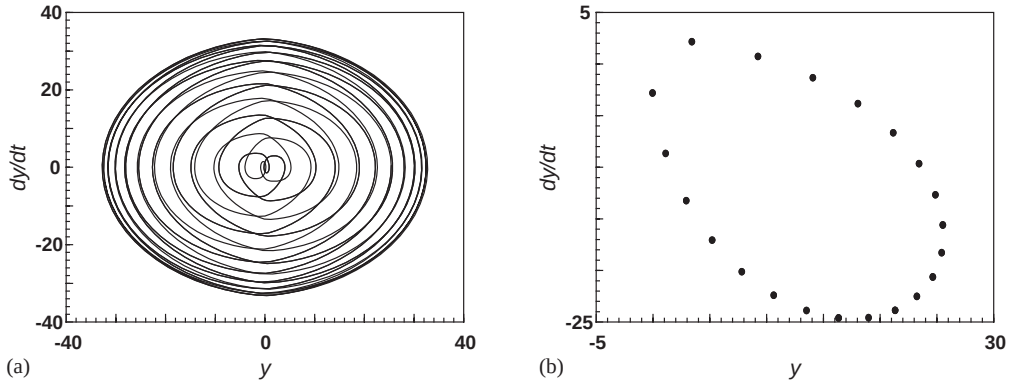

Fig. 4. The subharmonic motion of order 21: (a) phase portrait; (b) Poincaré section.

Only the stable double-crossing saturation region per cycle symmetric period-one solutions were found to exist at the excitation frequency in the region $\omega > (1+\omega_2^2)^{1/2}$, starting from any set of initial conditions. Besides symmetric period-one motions, a variety of asymmetric and subharmonic motions may be observed at some values of the excitation frequency out of the region; $\omega < 1$ or $1 \leqslant \omega \leqslant (1+\omega_2^2)^{1/2}$. The minimum period of a subharmonic motion, which is an integral multiple of the forcing period, indicates the order of the subharmonic motion. The Poincaré sections at different values of the excitation phase were used to sample the subharmonic motions to determine the order of a motion. The subharmonic motions of order two, three, four, five, six and seven were found to exist in some combinations of the system parameters. The subharmonic solutions seemed to disappear and period-one solutions to appear for higher damping levels. Some higher order subharmonic solutions were found to be sensitive to the calculation accuracy. A subharmonic motion of order 21, as shown in Fig. 4, was found to exist at $\delta = 0.0008$, $\omega_2 = \sqrt{3.2}$, $f = 5.25$, and $\omega = 0.96$.

Taking the excitation amplitude as the bifurcation parameter, a bifurcation diagram of the system response in the range $f \in [6.6, 7.8]$ under $\delta = 0.025$, $\omega_2 = \sqrt{5.0}$ and $\omega = 0.6$ is shown in Fig. 5(a). The sampled data onto the Poincaré section were at the excitation phase $\pi/2$. The diagram consists of three regular motion intervals $f \in [6.6, 7.143]$, $[7.244, 7.42]$ and $[7.57, 7.8]$, and two chaotic motion intervals $[7.143, 7.244]$ and $[7.42, 7.57]$. There exists a window of regular motions between the two chaotic motion intervals. The chaotic motions in the range $f \in [7.143, 7.244]$ result from typical period-doubling bifurcations, while the chaotic motions in $[7.42, 7.57]$ appear abruptly after a periodic motion loses its stability. The route to chaotic motions from period-doubling bifurcations is clearly illustrated in Fig. 5(b), an enlargement of the range $f \in [7.06, 7.18]$ from Fig. 5(a). Typical supercritical pitchfork bifurcations leading to a doubling period of the system motion appears at $f = 7.078$ and 7.132. A periodic solution is observed for $f \in [7.06, 7.078]$, a two-periodic solution for $[7.078, 7.132]$, and a four-periodic solution for $[7.132, 7.138]$. The chaotic motions seem to disappear after a reverse period-doubling bifurcation, stating from a chaotic motion to a two-periodic motion, and to a periodic motion. This may be seen in the parameter region $f \in [7.2, 7.4]$ from Fig. 5(a), which is enlarged in Fig. 5(c). A subcritical pitchfork bifurcation occurs at $f = 7.353$, where a period-two motion loses its stability

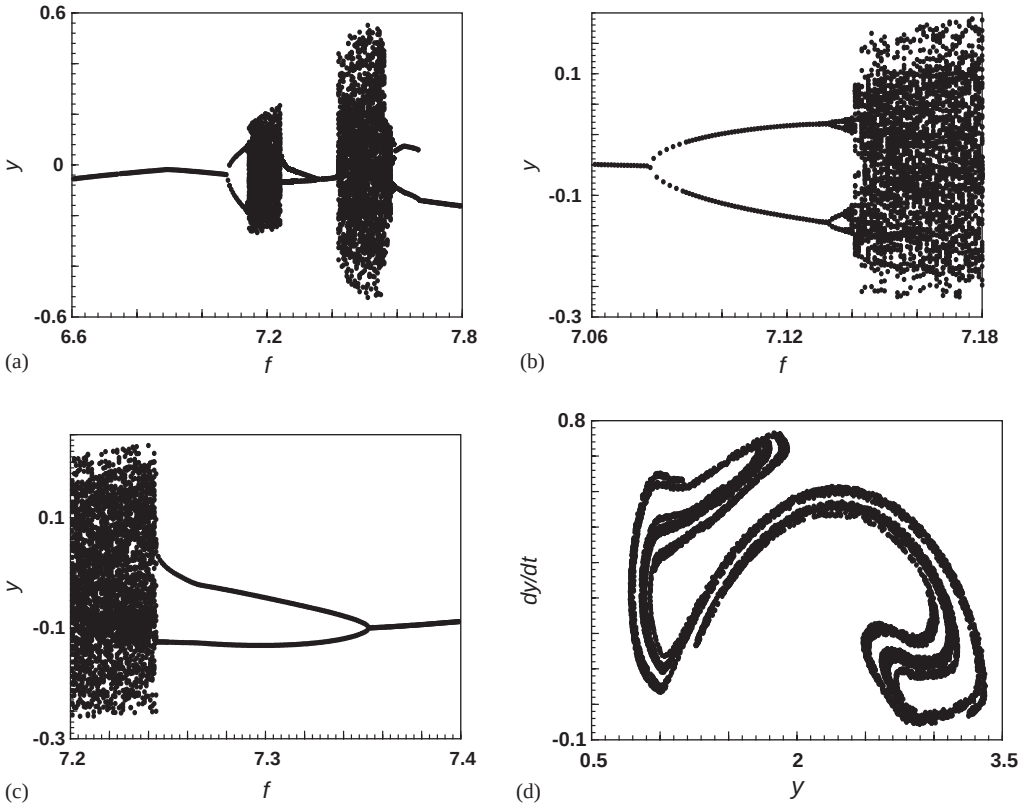

Fig. 5. The bifurcation diagrams of the system response under $\delta = 0.025$, $\omega_2 = \sqrt{5.0}$, $\omega = 0.6$, and the Poincaré map of a chaotic motion at $f = 7.2$.

and a period-one motion appears. Fig. 5(d) shows the Poincaré map of a regular chaotic attractor at $f = 7.2$ onto the phase of excitation $\pi/4$.

Another interesting dynamical behaviour, which widely exists in the system response, is a coexistence of different motions starting from different sets of initial conditions. Due to the extremely laborious calculations, a determination of the domain of attraction of various solutions is not considered in this paper. Only some examples are given instead. It has been found numerically that two, three, or even four stable solutions may coexist at some combinations of the system parameters. These multiple steady-state stable solutions starting from different sets of initial conditions were observed after the transient responses became negligible. In particular, it has been found that a double-crossing saturation region period-one motion became unstable and two double-crossing saturation region asymmetric stable solutions appeared. Each of two asymmetric solutions is the other's symmetric image about the origin, which is a property of the asymmetric solutions coexisting in this system. These asymmetric solutions result from a flip bifurcation of the symmetric solution, where it becomes unstable. In some combinations of the system parameters, a double-crossing saturation region symmetric stable motion may coexist with a subharmonic solution of order three or seven, as shown in Fig. 6. The motions shown in

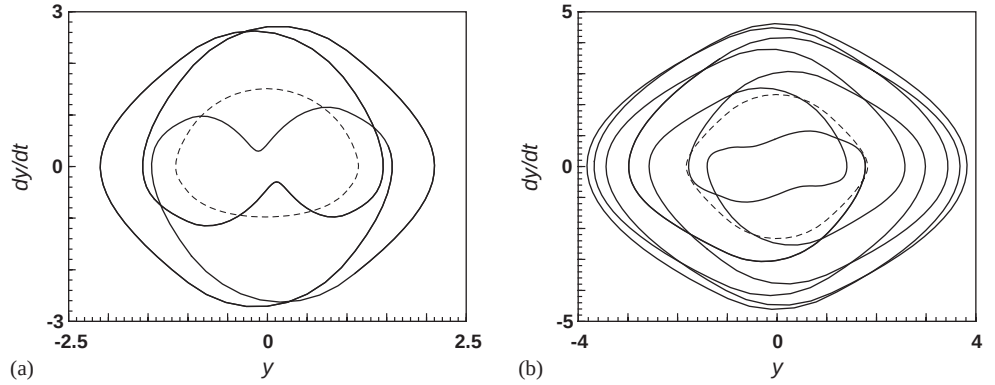

Fig. 6. The coexistence of a period-one motion (indicated by dashed curves) and a subharmonic motion of order (a) three; (b) seven.

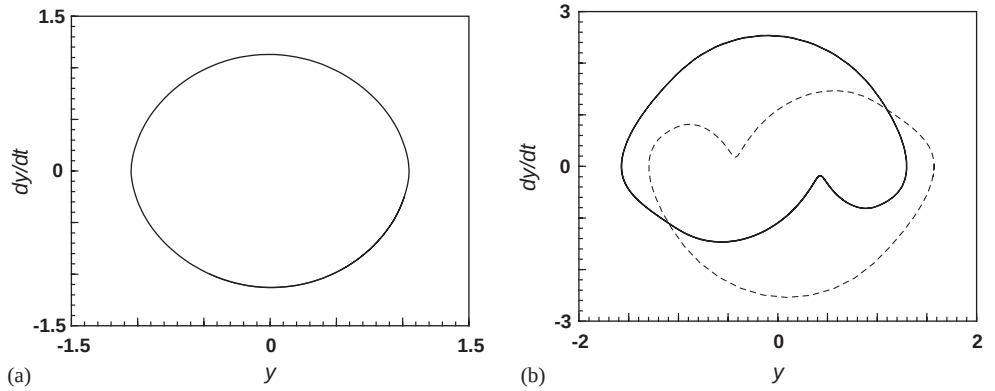

Fig. 7. The coexistence of a symmetric and two asymmetric double-crossing saturation region per cycle period-one solutions: (a) the symmetric solution; (b) two asymmetric solutions.

Fig. 6(a) were obtained using initial conditions $(0.1, 0.1)$ for the period-one motion and $(0.0, 1.0)$ for the subharmonic motion at the combination of the system parameters $\delta = 0.01$, $\omega_2 = \sqrt{3.6}$, $f = 4.0$ and $\omega = 0.98$. And the motions shown in Fig. 6(b) were obtained using initial conditions $(-0.1, -0.2)$ and $(1.0, 1.6)$ under $\delta = 0.01$, $\omega_2 = \sqrt{3.2}$, $f = 4.1$ and $\omega = 0.96$.

There also exist some combinations of the system parameters where three stable solutions coexist. For example, a double-crossing saturation region period-one solution may coexist with a pair of double-crossing saturation region asymmetric solutions, as shown in Fig. 7. These three solutions were obtained under the initial conditions $(1.8, 0.0)$, $(0.0, 1.0)$, and $(0.1, -0.2)$, respectively, for $\delta = 0.05$, $\omega_2 = \sqrt{5}$, $f = 5.3$ and $\omega = 1.0$. The asymmetric solutions also observe the property of the image symmetry. In addition, a pair of subharmonic motions of order three may coexist with a double-crossing saturation region symmetric motion, as shown in Fig. 8, at $\delta = 0.025$, $\omega_2 = \sqrt{4.98}$, $f = 5.8$ and $\omega = 1.0$. The initial conditions for these solutions are

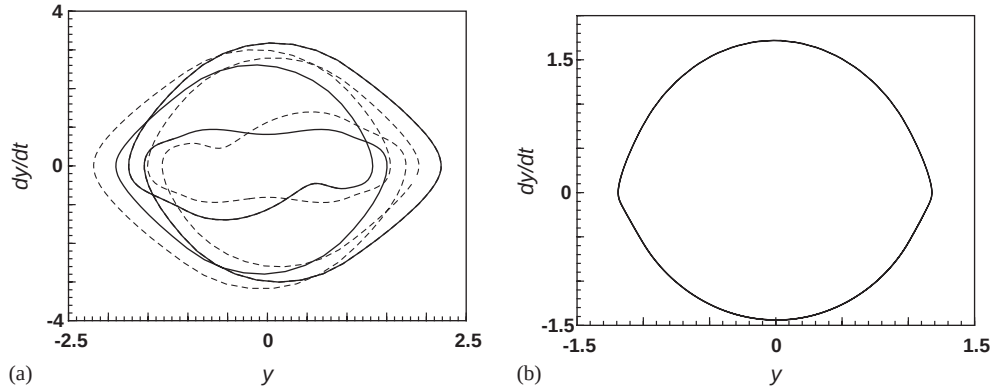

Fig. 8. The coexistence of a pair of subharmonic motions of order three and a symmetric period-one motion: (a) two subharmonic motions; (b) the period-one motion.

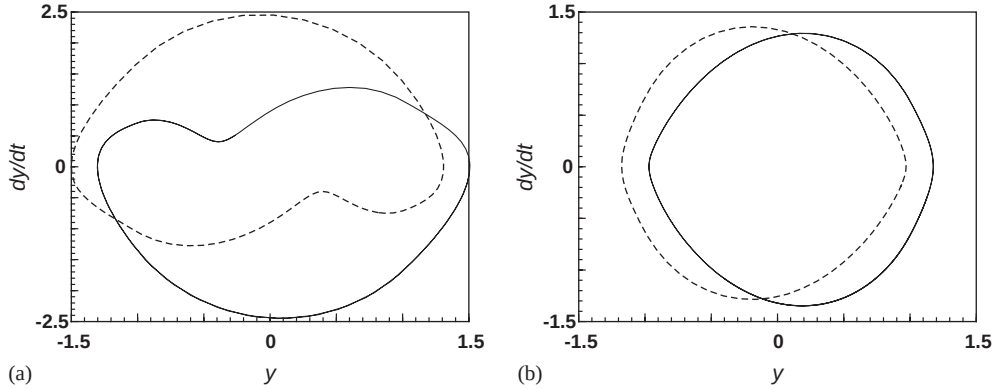

Fig. 9. The coexistence of a pair of double-crossing and a pair of single-crossing saturation region per cycle asymmetric period-one solutions: (a) two double-crossing solutions; (b) two single-crossing solutions.

$(0.1, -0.3)$, $(0.0, 1.0)$ and $(-0.2, -0.1)$ respectively. Each of the subharmonic motions is the other's symmetric image about the origin.

At certain combinations of the system parameters, a coexistence of four stable solutions was also found. For example, under $\delta = 0.05$, $\omega_2 = \sqrt{5}$, $f = 5.4$ and $\omega = 1.0$, a pair of asymmetric double-crossing saturation region solutions may coexist with a pair of single-crossing saturation region per cycle period-one solutions, as shown in Fig. 9. The initial conditions for the single-crossing saturation region solutions are $(1.8, 0.0)$ and $(0.0, -1.0)$, whereas those for the double-crossing solutions are $(0.0, 1.0)$ and $(-0.1, 0.1)$ respectively. Each of the asymmetric solutions is its companion's symmetric image about the origin.

A multiple-crossing saturation region per cycle period-one motion may also exist in the system response in the region $\omega < 1$. For example, there exists only a quadruple-crossing saturation region per cycle period-one solution starting from any set of initial conditions, at $\delta = 0.05$, $\omega_2 = \sqrt{2}$, $f = 3.2$ and $\omega = 0.5$.

6. Conclusions

In this paper, the dynamics of a periodically forced s.d.o.f. piecewise linear system has been investigated. The equations of motion, generalized from a practical engineering example, can also be used to model mathematically a class of linear controlled systems subjected to a saturation constraint and a periodic perturbation. A detailed analysis has been developed to obtain a double-crossing saturation region symmetric period-one solution. The stability of such a solution was determined by examining the asymptotic behaviour of the corresponding perturbed solutions. The system may also demonstrate other kinds of motions, namely asymmetric, subharmonic and chaotic motions. In addition, a coexistence of multiple stable solutions has been found using different sets of initial conditions.

Acknowledgements

This work has benefited from the support of the Alexander von Humboldt Foundation, Germany through the award of a research fellowship. The author is indebted to Professor R. Markert of the TU Darmstadt for his helpful discussion during the preparation of this manuscript, and for the hospitality he offered to the author during the author's stay in Germany. The author would also like to thank the anonymous referees for their useful comments on the manuscript.

References

[1] C.R. Fuller, S.J. Elliott, P.A. Nelson, *Active Control of Vibration*, Academic Press, London, 1996.
[2] G.F. Franklin, J.D. Powell, A. Emami-Naeini, *Feedback Control of Dynamic Systems*, 3rd Edition, Addison-Wesley, New York, 1994.
[3] G. Schweitzer, H. Bleuler, A. Traxler, *Active Magnetic Bearings, Basics, Properties and Application of Active Magnetic Bearings*, Verlag der Fachvereine (vdf), ETH-Zurich, 1994.
[4] S.W. Shaw, P.J. Holmes, A periodically forced piecewise linear oscillator, *Journal of Sound and Vibration* 90 (1983) 129–155.
[5] S. Natsiavas, Periodic response and stability of oscillators with symmetric trilinear restoring force, *Journal of Sound and Vibration* 134 (1989) 315–331.
[6] S.J. Hogan, On the dynamics of rigid-block motion under harmonic forcing, *Proceedings of the Royal Society of London A* 425 (1989) 441–476.
[7] S.J. Hogan, Damping in rigid block dynamics contained between side-walls, *Chaos, Solitons and Fractals* 11 (2000) 495–506.
[8] M. Wiercigroch, Modelling of dynamical systems with motion dependent discontinuities, *Chaos, Solitons and Fractals* 11 (2000) 2429–2442.
[9] S. Lenci, G. Rega, Periodic solutions and bifurcations in an impact inverted pendulum under impulsive excitation, *Chaos, Solitons and Fractals* 11 (2000) 2453–2472.
[10] D. Laier, R. Markert, Nonlinear oscillations of magnetically suspended rotors, *Proceedings of the Second European Nonlinear Oscillation Conference*, *Prague*, 1996, pp. 239–242.
[11] E.H. Maslen, P.E. Allaire, Magnetic bearing sizing for flexible rotors, *American Society of Mechanical Engineers Journal of Tribology* 114 (1992) 223–229.
[12] M.P. Karyeaclis, T.K. Caughey, Stability of a semi-active impact damper: part II, periodic solutions, *American Society of Mechanical Engineers Journal of Applied Mechanics* 56 (1989) 930–940.